Ultra Diffuse Galaxy formation constraints and possible detection in S-PLUS images

P. Astudillo Sotomayor[1], N.W.C. Leigh[1,2], R. Demarco[3], A.V. Smith Castelli[4,5], R.F. Haack[4,5], A.R. Lopes[4] & L.A. Gutierrez Soto[4]

[1] *Departamento de Astronomía, Universidad de Concepción, Chile*
[2] *Department of Astrophysics, American Museum of Natural History, EE.UU.*
[3] *Instituto de Astrofísica, Universidad Andrés Bello, Chile*
[4] *Instituto de Astrofísica de La Plata, CONICET–UNLP, Argentina*
[5] *Facultad de Ciencias Astronómicas y Geofísicas, UNLP, Argentina*

Received: 09 February 2024 / Accepted: 21 May 2024

Resumen / Presentamos trabajo preliminar asociado a la identificación de posibles escenarios de formación para las denominadas Galaxias Ultra Difusas (UDGs, por sus siglas en inglés) y sus sistemas de cúmulos globulares (GCs, por sus siglas en inglés). Para ello, ajustamos la función de luminosidad de los GCs, la cual se espera sea afectada por varios escenarios de formación. También presentamos nuestro plan de profundizar en el pasado colisional de las UDGs, estudiando las escalas de tiempo de fricción dinámica para acotar el tiempo transcurrido desde una posible interacción galaxia-galaxia. Por último, presentamos trabajo actualmente en desarrollo relacionado a la detectección de UDGs a la distancia del cúmulo de galaxias de Fornax en imágenes de la colaboración S-PLUS.

Abstract / We present preliminary work constraining possible formation scenarios for the formation of Ultra Diffuse Galaxies (UDGs) and the unique Globular Cluster (GC) populations some UDGs have. For this, we fit the GC luminosity function which is expected to be affected by several formation scenarios. We also present our plans to further delve into the collisional past of the UDGs, studying the GC dynamical friction timescale to constrain the time elapsed since a galaxy-galaxy interaction if this one occurred. We finally present our ongoing work attempting to detect UDGs at the Fornax cluster distance in images obtained by the S-PLUS collaboration.

Keywords / galaxies: dwarf — galaxies: star clusters: general — galaxies: formation — galaxies: luminosity function, mass function — galaxies: kinematics and dynamics

1. Introduction

Ultra diffuse galaxies (UDGs), as characterized by van Dokkum et al. (2015a), exhibit a distinctive combination of traits: low surface brightness ($\mu_e = 24 - 28$ mag arcsec^{-2}) akin to dwarf galaxies, coupled with significantly larger effective radii ($1.5 - 5$ kpc). They have been extensively observed across various environments, including galaxy clusters such as Coma and Virgo, as well as in groups and the field (van Dokkum et al., 2015a,b; Yagi et al., 2016; Koda et al., 2015; Mihos et al., 2015; González et al., 2018; Jones et al., 2023). These galaxies, characterized by old stellar populations and minimal ongoing star formation, typically reside on the red sequence of the color-magnitude diagram, with stellar masses ranging from 10^7 to 10^8 $M_\odot$ (Koda et al., 2015).

The origins of UDGs falls into two broad categories: in-situ and ex-situ processes. In the case of in-situ processes there's been numerous mechanism proposed such as stellar feedback and gas outflows Di Cintio et al. (2017); Chan et al. (2018), high momentum rotation of their haloes (Amorisco & Loeb, 2016; Benavides et al., 2023). Conversely, ex-situ mechanisms, predominant in dense environments like galaxy clusters, involve external forces such as ram-pressure stripping and tidal interactions, which strip galaxies of their gas reservoirs (Martin et al., 2019). Other scenarios propose UDGs to be "failed galaxies" with Milky Way-like dark matter haloes but stellar masses corresponding to the dwarf galaxy range (e.g. Janssens et al., 2022; Toloba et al., 2023).

Carleton et al. (2019) proposed that the tidal stripping of dwarf galaxies with cored halos better reproduces observed UDG properties, particularly in cluster environments. However, discrepancies remain, particularly in explaining extremely large UDGs and those experiencing significant mass loss. Recent studies, including those by van der Burg et al. (2017) and Carleton et al. (2021), suggest an increase in UDG abundance with host cluster mass, indicative of a correlation with environment. Notably, observations of globular clusters in UDGs like NGC1052-DF2 and NGC1052-DF4 (hereafter DF2 and DF4) support a top-heavy GC Luminosity Function (GCLF) in various environments.

Our study aims to bring hints to which formation mechanism is more likely to create UDGs by studying their GCs populations in different environments. We

✉ *Contact* / pastudillo2018@udec.cl

present an initial sample from diverse environments and outline our methodology for studying GC populations. Additionally, we discuss the implications of our work in the broader context of the S-PLUS Fornax Project (S+FP; Smith Castelli et al., 2024).

2. Methodology and Results

We use publicly available catalogs of GCs in the UDGs and properties of the host galaxies reported in the literature, such as effective radius, stellar mass, Sérsic index and mean surface brightness in the F814W filter to perform our analysis in the GCs populations. This parameters are listed in Table 1. All the other parameters are derived or estimated as explained in the subsequent sub-sections. In Section 2.1 we show the fit of skewed gaussian functions to the GCLF of the UDGs. In Section 2.2, we calculate the radial profiles for mass, density and velocity dispersion fitting observable parameters to theoretical functions. In Section 2.3 we estimate the effective mass-to-light ratio using a function dependent in $\log \sigma$ and $\log I_e$ (see Zaritsky & Behroozi 2022). Finally, in Section 2.4 we calculate dynamical friction timescales for all GCs in the UDGs.

2.1. Globular Cluster Luminosty Function

The GCLF has been historically described as a gaussian with a near universal peak at $M_V \approx -7.5$ Harris & van den Bergh (1981) First, we fit skewed Gaussian functions to the GCLF histograms of each UDG. For this, we build a kernel density estimation of the data using the python package SCIKIT-LEARN (Pedregosa et al., 2011), opting for a Gaussian kernel. After this, we retrieve the parameters for a skewed Gaussian probability density function (SCIPY;Virtanen et al. 2020) using the negative log-likelihood function. Most UDGs like those in the Coma cluster and DGSAT-I show a turnover magnitude (M_0^T) consistent with the Universal peak $M_{I,0} \approx -8.4$ mag described by Harris & van den Bergh (1981). DF2 and DF4 are the only outliers to this universal property pointing to the idea that they should have a formation scenario completely different from other UDGs. We summarize the skewed Gaussian parameters in Table 2.

2.2. Radial profiles

To calculate the dynamical friction timescales for all GCs in our UDGs, first we need to compute numerically the mass, density and velocity dispersion profiles. The mass enclosed within a radius r is required to calculate the density and velocity dispersion profiles. This is done by fitting observational parameters such as the Sérsic index, n, and the effective surface brightness, I_e. Following Leigh & Fragione (2020) and Terzić & Graham (2005), we define:

$$\rho_0 = \frac{\sqrt{\pi}}{4R_e} \Upsilon_0 I_e b^{n(1-p)}, \tag{1}$$

where Υ_0 is the mass-to-light ratio. The variables b and p are approximated as:

$$b = 1.9992n - 0.3271 \tag{2}$$

$$p = 1 - \frac{0.6097}{n} + \frac{0.055}{n^2}. \tag{3}$$

The mass profile is equation (A2) from Terzić & Graham (2005):

$$M(r) = 4\pi\rho_0 R_e^3 n b^{n(p-3)} \gamma(n(3-p), z) \tag{4}$$

For the density profile, we assume an isotropic and spherical distribution of mass:

$$\rho(r) = \frac{M(r)}{4/3\pi r^3}. \tag{5}$$

Finally, the velocity dispersion profile follows equation (A5) from Terzić & Graham (2005) which is the numerical solution of:

$$\sigma_s^2(r) = \frac{G}{\rho(r)} \int_r^\infty \rho(\bar{r}) \frac{M(\bar{r})}{\bar{r}^2} d\bar{r}. \tag{6}$$

2.3. Mass-to-light ratio estimation

The mass-to-light ratios are estimated using the following equation, with parameters $a = 0.198$, $b = 0.140$, $c = 0.192$, $d = -0.923$, $e = -0.108$ and $f = 1.306$ obtained by Zaritsky & Behroozi (2022) from fitting elliptical and dwarf elliptical galaxies, UDGs, dwarf spheroidal and ultra-faint satellites of the Milky Way and M31, and compact dwarf galaxies:

$$\log \Upsilon_e = a\,(\log\sigma)^2 + b \log\sigma + c\,(\log I_e)^2 + d \log I_e + e \log I_e \log\sigma + f. \tag{7}$$

2.4. Dynamical friction timescales

Following the treatment performed by Leigh & Fragione (2020) for DF2 and DF4, we study the past collisional evolution of observed GC populations, starting with the calculation of the dynamical friction (DF) timescales of each GC. DF timescales shorter than a Hubble time will motivate formation scenarios where the GC populations have had sufficient time to have their orbits become more centrally concentrated. The present-day positions of the GCs are in such cases not where they formed in their host galaxy.

The DF timescale (τ_{DF}) assuming circular orbits is given by (Binney & Tremaine, 1987; Gnedin et al., 2014):

$$\tau_{DF} = \frac{1.17\, M(r)\, r}{\ln\Lambda\, m_{GC}\, \sigma(r)} \tag{8}$$

As seen in Fig. 1, all GCs within $r \lesssim 3$ kpc for the UDGs in the sample, display DF timescales shorter than a Hubble time. Janssens et al. (2022) found the GC system of DGSAT-I to be more compact than the galaxy $R_{GC}/R_e = 0.7$. The compact GC system of DGSAT-I is consistent with what we find. This could be explained by the low DF timescales, such that the spatial distribution of the GC population in DGSAT-I was normal at birth, in comparison to the ones of other galaxies in our sample.

Table 1. UDGs parameters obtained from the literature.Column (2) present the filters in which the UDGs were observed, column (3) shows the number of GCs in each UDG, column (4) presents the stellar mass in solar masses, in column (5) we show the effective radius, column (6) lists the effective surface brightness in magnitudes per arcsecond, and columns (7) and (8), the Sérsic index and the environment where the UDG is located, respectively. * indicates that the galaxy is located in the outskirts of the Coma cluster. ** indicates that the galaxy is located in a filament of the Pisces-Perseus Supercluster, but isolated from groups or clusters. The references from which the listed values were obtained are shown in column (9) and are as follows: (a)Montes et al. (2021),(b) van Dokkum et al. (2018), (c) Montes et al. (2020), (d)van Dokkum et al. (2019), (e)Saifollahi et al. (2022), (f) Janssens et al. (2022).

Galaxy	Filters	N_{gc}	M_* ($M_\odot$)	r_e (kpc)	$< \mu >_{e,F814W}$ (mag arcsec^{-1})	n	Env.	ref
(1)	(2)	(3)	(4)	(5)	(6)	(7)	(8)	(9)
NGC1052-DF2	F606W, F814W	14	2.0×10^8	2.20	25.24	0.55	Group	(a),(b)
NGC1052-DF4	F606W, F814W	11	1.5×10^8	1.60	25.06	0.79	Group	(c),(d)
DF07	F475W, F814W	17	2.8×10^8	3.74	24.69	0.81	Cluster	(e)
DF08	F475W, F814W	10	0.6×10^8	3.07	25.61	0.88	Cluster	(e)
DF17	F475W, F814W	24	1.4×10^8	3.75	25.34	0.65	Cluster	(e)
DF44	F475W, F814W	22	2.1×10^8	4.21	25.08	0.77	Cluster	(e)
DFX1	F606W, F814W	19	1.5×10^8	3.73	25.10	0.92	Cluster	(e)
SMDG1251014	F475W, F814W	30	4.9×10^8	5.06	25.20	1.01	Cluster*	(e)
DGSAT-I	F606W, F814W	12	3.3×10^8	4.70	25.00	0.38	Isolated**	(f)

Table 2. Results from fitting a skewed Gaussian function to the GCLF of the UDGs in the sample presented in Table 1. Columns (2), (3) and (4) are the skewed Gaussian parameters obtained from the fitting of the GCLF in the filter F814W. They are, from left to right, the peak magnitude, the standard deviation and the skewness parameter, respectively.

Galaxy	M_0^T [mag]	σ	α
(1)	(2)	(3)	(4)
DF2	-9.32 ± 0.01	0.77 ± 0.20	1.13
DF4	-9.33 ± 0.00	0.80 ± 0.24	1.29
DF07	-8.61 ± 0.03	0.92 ± 0.22	-0.30
DF08	-8.16 ± 0.02	0.69 ± 0.22	-0.18
DF17	-7.99 ± 0.02	0.84 ± 0.17	-2.50
DF44	-7.65 ± 0.03	1.13 ± 0.24	-5.18
DFX1	-8.12 ± 0.03	0.65 ± 0.15	-1.19
SMDG1251014	-8.34 ± 0.03	0.90 ± 0.17	-1.90
DGSAT-I	-8.22 ± 0.06	1.33 ± 0.38	-2.81

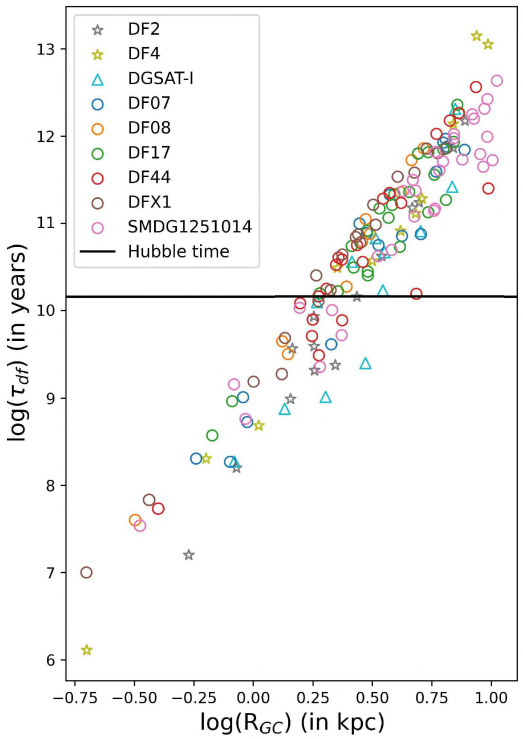

Fig. 1. DF timescales (in years) as a function of projected galactocentric distance (in kpc). Circles represent GCs in UDGS in the Coma cluster, triangles represent GCs in the isolated UDG DGSAT-I and stars show GCs in NGC1052-DF2 and NGC1052-DF4. The solid horizontal line depicts a Hubble time.

3. Ultra Diffuse Galaxies in the Fornax Cluster using S-PLUS

In order to better constrain our previous results, we look for significantly enlarge our sample of GCs in UDGs placed in dense environments. To that aim, we have been able to detect UDGs, previously observed in the context of the *Systematically Measuring Ultra Diffuse Galaxies* (SMUDGes) project (Zaritsky et al. 2019, 2023), in S-PLUS images that are being analyzed as part of the S-PLUS Fornax Project (S+FP; Smith Castelli et al. 2024) (Fig. 2). The S+FP aims at studying the galaxy and GC populations in the Fornax cluster and its surroundings, using 106 S-PLUS fields (1.4×1.4 deg^2) which cover an area of ≈ 208 deg^2. With this coverage, the S+FP reaches up to $5 \times R_{vir}$ in RA. Previous studies focused on low surface brightness (LSB) galaxies and UDGs in Fornax, such as those performed by the Next Generation Fornax Survey (NGFS; Muñoz et al. (2015)) and the Fornax Deep Survey (FDS; Venhola et al. 2017, 2022), have mostly been concentrated in the inner region of the cluster (≈ 1 R_{vir}). However, SMUDGes, encompassing $\approx 14,000$ deg^2 of the sky, provides us with UDG candidates covering, in projection, all S+FP fields. The well-populated sample of already known UDGs in For-

nax, will allow us to significantly extend our study of the UDGs' GC systems in a rich nearby cluster. It is worth noticing that S-PLUS will only allow us to study the bright end of the GCLF (see Section 3.11.1 in Smith Castelli et al. 2024). However, considering that for most UDGs (with exception of DF2 and DF4) the GCLF is consistent with the expected reuniversal GCLF, at least in peak magnitude, we will still be able to reconstruct their GCLF. We are starting to deepen in such an analysis and we expect to submit a paper with the results soon.

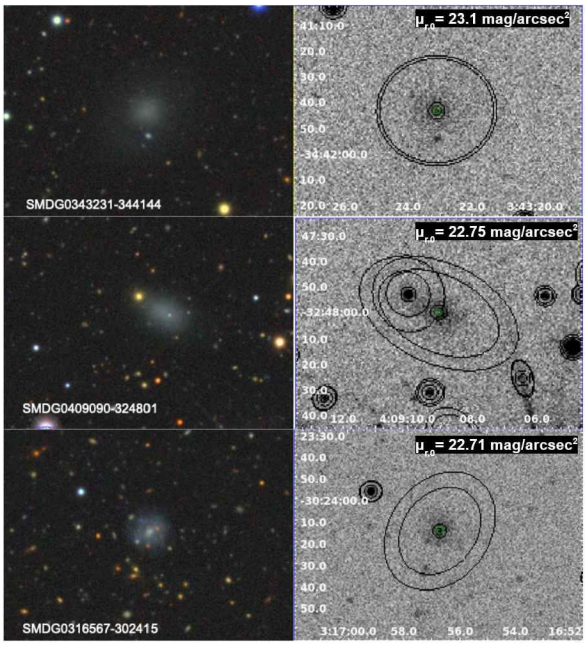

Fig. 2. Three UDGs previously identified by SMUDGes in the Fornax cluster, that have been recently detected with SExtractor in S-PLUS images. The left panel shows the galaxy images obtained from the DESI Legacy Imaging Survey and, the right panel, the detection by SExtractor using RUN 2 from Haack et al. (2024)

Acknowledgements: We acknowledge funding from ANID, Chile via Millenium Nucleus NCN23_002 (TITANs) and BASAL FB210003 NWCL gratefully acknowledges the generous support of a Fondecyt General grant 1230082, as well as support from Núcleo Milenio NCN2023_002 (TITANs) and funding via the BASAL Centro de Excelencia en Astrofisica y Tecnologias Afines (CATA) grant PFB-06/2007. NWCL also thanks support from ANID BASAL project ACE210002 and ANID BASAL projects ACE210002 and FB210003. RD also gratefully acknowledges support by the ANID BASAL project FB210003. A.V.S.C., R.F.H., A.R.L. and L.A.G.S. acknowledge financial support from CONICET, Agencia I+D+i (PICT 2019-03299) and Universidad Nacional de La Plata (Argentina). S-PLUS is an international collaboration founded by Universidade de Sao Paulo, Observatório Nacional, Universidade Federal de Sergipe, Universidad de La Serena and Universidade Federal de Santa Catarina.

References

Amorisco N.C., Loeb A., 2016, MNRAS, 459, L51
Benavides J.A., et al., 2023, MNRAS, 522, 1033
Binney J., Tremaine S., 1987, *Galactic dynamics*
Carleton T., et al., 2019, MNRAS, 485, 382
Carleton T., et al., 2021, MNRAS, 502, 398
Chan T.K., et al., 2018, MNRAS, 478, 906
Di Cintio A., et al., 2017, MNRAS, 466, L1
Gnedin O.Y., Ostriker J.P., Tremaine S., 2014, ApJ, 785, 71
González N.M., et al., 2018, A&A, 620, A166
Haack R.F., et al., 2024, MNRAS, 530, 3195
Harris W.E., van den Bergh S., 1981, AJ, 86, 1627
Janssens S.R., et al., 2022, MNRAS, 517, 858
Jones M.G., et al., 2023, ApJL, 942, L5
Koda J., et al., 2015, ApJL, 807, L2
Leigh N.W.C., Fragione G., 2020, ApJ, 892, 32
Martin G., et al., 2019, MNRAS, 485, 796
Mihos J.C., et al., 2015, ApJL, 809, L21
Montes M., et al., 2020, ApJ, 904, 114
Montes M., et al., 2021, ApJ, 919, 56
Muñoz R.P., et al., 2015, ApJL, 813, L15
Pedregosa F., et al., 2011, Journal of Machine Learning Research, 12, 2825
Saifollahi T., et al., 2022, MNRAS, 511, 4633
Smith Castelli A.V., et al., 2024, MNRAS
Terzić B., Graham A.W., 2005, MNRAS, 362, 197
Toloba E., et al., 2023, ApJ, 951, 77
van der Burg R.F.J., et al., 2017, A&A, 607, A79
van Dokkum P., et al., 2018, Nature, 555, 629
van Dokkum P., et al., 2019, ApJL, 874, L5
van Dokkum P.G., et al., 2015a, ApJL, 798, L45
van Dokkum P.G., et al., 2015b, ApJL, 804, L26
Venhola A., et al., 2017, A&A, 608, A142
Venhola A., et al., 2022, A&A, 662, A43
Virtanen P., et al., 2020, Nature Methods, 17, 261
Yagi M., et al., 2016, ApJS, 225, 11
Zaritsky D., Behroozi P., 2022, MNRAS, 519, 871
Zaritsky D., et al., 2019, ApJS, 240, 1
Zaritsky D., et al., 2023, ApJS, 267, 27